DOAS measurement of glyoxal as an indicator for fast VOC chemistry in urban air

Rainer Volkamer, Luisa T. Molina, and Mario J. Molina

Department of Earth, Atmospheric, and Planetary Sciences, Massachusetts Institute of Technology, Cambridge, Massachusetts, USA

Terry Shirley and William H. Brune

Department of Meteorology, Pennsylvania State University, University Park, Pennsylvania, USA

[1] We present the first direct measurements of glyoxal (CHOCHO) in the atmosphere, and demonstrate that glyoxal measurements are possible by differential optical absorption spectroscopy (DOAS). Glyoxal was routinely detected during the daytime in Mexico City, where mixing ratios ranged from <0.15 ppbv (detection limit) to 1.82 ppbv. These time-resolved measurements resolve the rapid diurnal variation of glyoxal, and indicate the onset of volatile organic compound (VOC) oxidation about 1hr after sunrise. The atmospheric lifetime of glyoxal is determined to be 1.3 hr for overhead sun conditions. Then elevated glyoxal levels indicate a persistently active VOC chemistry during most of the day. Glyoxal forms from the oxidation of numerous VOCs, which foster the formation of 'photochemical smog' including ozone and aerosol particles; atmospheric levels are essentially unaffected by direct vehicle emissions in Mexico City. Satellite measurements of glyoxal seem feasible, making possible the better identification of photochemical hot spots in the Earth's atmosphere. **Citation:** Volkamer, R., L. T. Molina, M. J. Molina, T. Shirley, and W. H. Brune (2005), DOAS measurement of glyoxal as an indicator for fast VOC chemistry in urban air, *Geophys. Res. Lett.*, *32*, L08806, doi:10.1029/2005GL022616.

1. Introduction

[2] In many large cities opportunities for a better quality of life are offset by a severe degradation of air quality caused by photochemical smog [*Finlayson-Pitts and Pitts*, 2000], which causes adverse effects on human health [*Molina and Molina*, 2002], agriculture [*Gregg et al.*, 2003], and regional climate [*Ramanathan et al.*, 2001]. While the crucial role of volatile organic compounds (VOCs) in the formation of photochemical smog is well established [*Finlayson-Pitts and Pitts*, 2000; *Molina and Molina*, 2002], the development of robust control strategies to reduce ozone (O_3) and aerosol levels in urban air requires the identification and measurement of molecules that indicate the rate of VOC oxidation. In urban air, the performance of traditional VOC oxidation indicators like O_3, O_x (sum of O_3 and nitrogen dioxide (NO_2)), formaldehyde (HCHO), and methylvinylketone (MVK) is affected by direct vehicle emissions [*Finlayson-Pitts and Pitts*,

2000], which contribute significantly to the atmospheric concentrations of these species; in the case of O_3, high concentrations of nitric oxide (NO) efficiently scavenge this gaseous pollutant during morning rush hour. Thus, atmospheric concentrations of these trace gases may be ambiguous indicators for VOC chemistry in urban air.

[3] Glyoxal (CHOCHO), the smallest α-dicarbonyl, is a mutagenic product [*Kielhorn et al.*, 2004] formed from the oxidation of numerous VOCs [*Calvert et al.*, 2000; *Volkamer et al.*, 2001; *Calvert et al.*, 2002]; minor amounts have further been reported in tailpipe emissions [*Grosjean et al.*, 2001; *Kean et al.*, 2001]. During the day, photolysis and reaction with OH-radicals determine its atmospheric residence time [*Atkinson*, 2000]. We present the first direct measurement of glyoxal in the atmosphere, and experimentally quantify its atmospheric lifetime in Mexico City.

2. Instrument and Data Analysis

[4] We used Long-Path DOAS (LP-DOAS) to detect glyoxal by its unique specific narrow-band (<5 nm) absorption structures in the visible spectral range, that enable DOAS [*Platt*, 1994] to separate trace gas absorptions from broadband molecule and aerosol extinction in the open atmosphere. Measurements were taken as part of the MCMA-2003 field campaign, which was held during spring 2003 in the Mexico City Metropolitan Area (MCMA). Two LP-DOAS instruments were deployed on the roof of the National Center for Research and Training (Centro Nacional de Investigación y Capacitación Ambiental, CENICA). Only data from DOAS#2 is described here; a similar instrument is described by *Alicke et al.* [2003]. An array of retroreflectors was placed at Museo Fuego Nuevo (Cerro de la Estrella) resulting in a total atmospheric light-path of 4420 m on average 70 m above ground. Atmospheric spectra were recorded by sequentially projecting 80-nm wide wavelength intervals onto the 1024-element PDA; background spectra recorded within a few minutes were subtracted to correct for stray-light from the atmosphere. Glyoxal was retrieved every 2–15 min from evaluating the spectral range between 420 and 465 nm, using non-linear least squares fitting of glyoxal, NO_2, O_4, H_2O, two lamp-reference spectra, and a 5th order polynomial high pass filter and the Windoas software [*Fayt and van Roozendael*, 2001]. As reference spectra available high-resolution absorption cross-section spectra [see, e.g., *Alicke et al.*, 2003] were degraded to our instrument resolution (ca. 0.4 nm FWHM). Glyoxal is
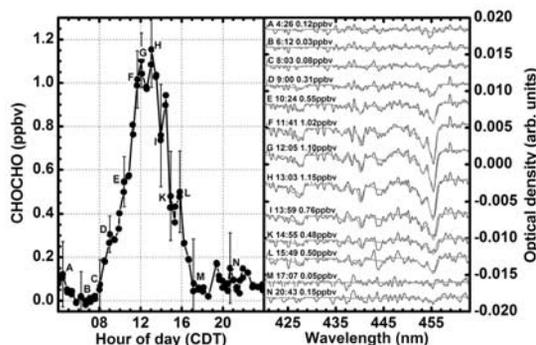
Figure 1. Concentration time profile of glyoxal measured on 10 April 2003. Letters indicate atmospheric spectra shown on the right (thin lines) after removal of trace-gas absorptions other than glyoxal and Xe-emission lines; scaled glyoxal references spectra are overlayed (thick lines); error bars indicate the absolute 2-sigma uncertainty. The maximum glyoxal absorption (4.9×10^{-3}) is representative for typical campaign days. See color version of this figure in the HTML.

inherently calibrated from knowledge of its differential absorption cross-section [*Volkamer et al.*, 2005], which for the three covered lines was 5.5, 2.5, and 1.7×10^{-19} cm^2 at 455, 440, and 428 nm, respectively. Absorption features with differential optical densities of 8×10^{-4} could be detected, corresponding to a mean detection limit of 3×10^9 molec/cm^3 or 0.15 ppbv (1 ppbv = 1 parts per billion by volume = 1.92×10^{10} molec/cm^3 at 295 K and 783 mbar). Besides CHOCHO, DOAS#2 also measured HCHO, HONO, NO$_2$, O$_3$, and SO$_2$; only selected data are presented here.

[5] Photolysis frequencies of CHOCHO (J$_{CHOCHO}$) and other trace gases were measured by spectroradiometry. The spectroradiometer measured solar actinic flux spectra from 280 nm to 450 nm with a spectral band pass of 1 nm. The step width was set to 2 nm below 320 nm, and 5 nm above. The radiation from the upper hemisphere was collected by a diffuser optic with almost uniform sensitivity for all angles of incidence within a solid angle of 2πsr. A Bentham DMc 150 double monochromator equipped with a tuneable grating (2400 grooves/mm) was used for wavelength dispersion and a photomultiplier for photon detection. The actinic flux calibration of the spectroradiometer was performed before and after the campaign at the Forschungszentrum Juelich in Germany using certified irradiance standards as described by *Kraus et al.* [2000]. J-values for CHOCHO were calculated using absorption cross-sections and quantum yields as described in [*Volkamer et al.*, 2005], and multiplied by 1.1 to account for surface albedo.

[6] OH was measured with laser-induced fluorescence (LIF) in detection chambers at low pressure, a technique commonly referred to as FAGE. With this technique, air is drawn into a low-pressure chamber by a vacuum pump. As the air passes through the detection chamber, OH is excited by a laser that is tuned to the wavelength of an OH electronic transition near 308 nm; the fluorescence from the excited OH is detected with a time-gated microchannel plate (MCP) detector. During MCMA-2003, the OH detection chamber was mounted on a tower 6 m above the roof of

the CENICA building; the laser and electronics were housed in the rooftop laboratory with the DOAS instruments. A full description of the technique and instrument is given by *Faloona et al.* [2004].

3. Results and Discussion

[7] Glyoxal was detected on all days of the campaign. The highest optical density of glyoxal absorption was 8.5×10^{-3}, corresponding to a concentration of $(3.5 \pm 0.3) \times 10^{10}$ molec/cm^3 or (1.82 ± 0.15)ppbv. The value and the time of glyoxal peak concentrations varied from day to day, but concentrations generally increased steeply about 1hr after sunrise (7 am central daylight savings time = CDT = UTC−5h); peaked 1−4 hr before solar noon (1:45 pm); remained detectable for most of the day; and typically dropped to levels close to the detection limit few hours before sunset (Figure 1). Virtually no glyoxal was detected during most nights, and concentrations were below the detection limit during early morning hours. A recent report by the World Health Organization compiled indirect glyoxal measurements by cartridge collection/chromatography methods [*Kielhorn et al.*, 2004]; concentrations range between 0.04 to 4.1 ppbv in rural and urban atmospheres. Glyoxal levels in the MCMA are well within this range, and indeed do not seem exceptionally high, suggesting that routine DOAS measurements of glyoxal are feasible in other locations.

[8] The repeating pattern of steeply rising glyoxal concentrations shortly after sunrise gives insight into glyoxal sources in urban air (Figure 2). In the MCMA, one of the world's largest cities and a case study for other cities in the developing world, ~50% of VOC and ~80% of NO$_x$ (sum of NO and NO$_2$) emissions are due to vehicles [*Molina*
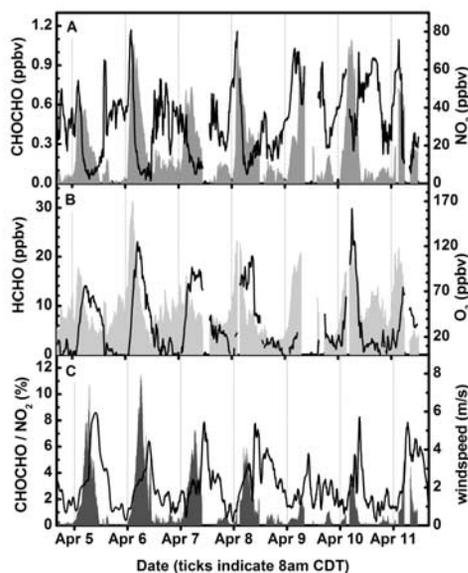

Figure 2. Time series of CHOCHO, HCHO, NO$_2$, O$_3$ mixing ratios and wind speed. (a) Glyoxal (shaded area), NO$_2$ (solid line); (b) HCHO (shaded area), O$_3$ (solid line); (c) the glyoxal-to-NO$_2$ ratio (shaded area) and wind speed (solid line). Tick marks indicate about 1 hr after sunrise. See color version of this figure in the HTML.
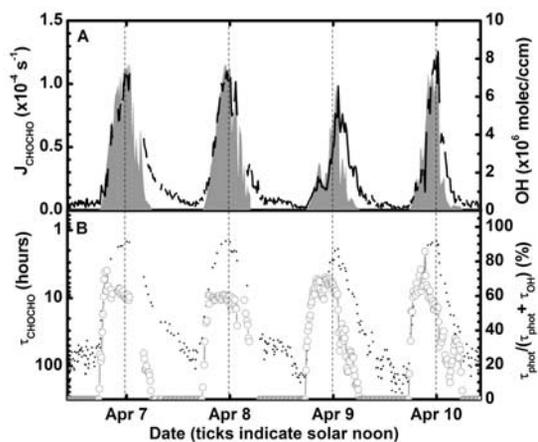
Figure 3. Atmospheric lifetime of glyoxal with respect to photolysis and OH-radical initiated loss. (a) J_{CHOCHO} (shaded area), OH-radical concentrations (solid line); (b) $\tau_{CHOCHO} = 1/(k_{OH+CHOCHO} \times OH + J_{CHOCHO})$ (dotted line), and portion of photolytic loss (open dots). See color version of this figure in the HTML.

and Molina, 2002]; increasing NO_2 concentrations before sunrise are traffic related. Glyoxal concentrations remained below the detection limit before sunrise, indicating that atmospheric glyoxal levels are essentially unaffected by tailpipe emissions (Figure 2a). A semi-quantitative assessment of primary CHOCHO sources confirms this observation: the molar emission ratio of HCHO relative to that of CHOCHO was measured to be ~40 (heavy-duty-diesel), ~730 (gasoline), and ~200 (US mix of diesel and gasoline powered light-duty vehicles) [*Kean et al.*, 2001; *Grosjean et al.*, 2001]. With about two third of fuel sales in the MCMA being gasoline [*Molina and Molina*, 2002], average molar CHOCHO emissions are expected at least two orders of magnitude lower than those of HCHO. Primary emissions of HCHO contribute <8 ppbv HCHO accumulation overnight (Figure 2b); corresponding CHOCHO emissions may account for 50 pptv or less CHOCHO in the morning atmosphere. This is below the detection sensitivity of our setup, and corroborates that alternative sources of glyoxal determine the diurnal variation of glyoxal. With CHOCHO being about 20 times less abundant than HCHO in the MCMA, CHOCHO concentrations are about an order of magnitude less affected by primary sources than those of HCHO, as is also reflected in the larger diurnal variability of CHOCHO (Figure 2).

[9] The atmospheric lifetime of glyoxal τ_{CHOCHO} with respect to photolysis and reaction with OH-radicals is assessed in Figure 3. J_{CHOCHO} and OH-radical concentrations (Figure 3a) were used to calculate the lifetime of glyoxal, assuming $k_{OH+CHOCHO} = 1.1 \times 10^{-11}$ cm^3/molec/s [*Plum et al.*, 1983]. The glyoxal lifetime with respect to these gas-phase loss-processes was longest (several 100 hr) during morning rush hour (before sunrise), somewhat lower at night ($\tau_{night} \approx 50$ hr), and decreased rapidly after sunrise to reach minimum values $\tau_{min} \approx 1.3$ hr for overhead sun (solar zenith angle, $SZA = 10°$). This atmospheric lifetime of glyoxal is about four times shorter compared to previous estimates [*Atkinson*, 2000] reflecting recent updates in

photochemical parameters of glyoxal photolysis. For a 'cloudless' day in the MCMA, the average daytime lifetime of glyoxal was $\tau_{day} \approx 2.2$ hr ($SZA < 60°$).

[10] A distinct diurnal variation is observed in the relative importance of OH-radical initiated and photolytic loss of glyoxal (Figure 3b). In the early morning hours ($SZA > 80°$) glyoxal loss is largely determined by reactions with OH-radicals. Photolytic loss rapidly gains importance towards lower SZAs, and dominates photochemical loss for most of the day. The portion of photolyic glyoxal loss then is surprisingly constant (Figure 3b), and for 'cloudless' days accounts for about 60–75% of gas-phase glyoxal losses. During most afternoons clouds were observed, causing OH-reactions to gain relative importance. The effect of NO_3-radicals on glyoxal lifetime can be assessed assuming the rate constant for the NO_3-radical reaction with glyoxal as twice that of HCHO [*Sander et al.*, 2002], i.e. $k_{NO3+CHOCHO} = 1.16 \times 10^{-15}$ cm^3/molec/s, and calculating an upper limit for the NO_3-radical concentration as $NO_3 < NO_2 \times O_3 \times k_{NO2+O3}/(NO \times k_{NO+NO3})$, where NO_2 and O_3 are measured concentrations (Figure 2) in units molec/cm^3, $k_{NO2+O3} = 3.2 \times 10^{-17}$ cm^3/molec/s, $k_{NO+NO3} = 2.6 \times 10^{-11}$ cm^3/molec/s are the rate constants for the NO_3-source reaction of NO_2 with O_3, and the NO_3-sink reaction with NO [*Sander et al.*, 2002]. Assuming $NO = 1$ ppbv, and neglecting further NO_3-sinks from photolysis, N_2O_5 hydrolysis or reactions with VOCs, the steady-state NO_3-radical concentration is expected <5 pptv during the campaign. Such NO_3-radical concentration would affect glyoxal lifetime by 0.3% in the late afternoon (5–8 pm, $\tau_{CHOCHO} \approx 8$ hr) and 2% during the night. NO_3-radical initiated loss – if at all important – is a very minor glyoxal sink in urban air, where OH-radical initiated loss is the dominant gas-phase sink at night. Additional glyoxal losses from dry deposition and transfer to aerosols are expected [*Jang et al.*, 2002; *Kalberer et al.*, 2004], but too little information is as yet available to assess the relevance of these sinks for atmospheric residence times.

[11] The rapid increase of CHOCHO shortly after sunrise reveals a very efficient VOC oxidation process during morning hours (Figure 2). The maximum accumulation rate of glyoxal varied between 0.24–0.89 ppbv/hr for different days (campaign average of 0.49 ppbv/hr between 8–10 am). A nearly simultaneous rise in NO_2 is consistent with the reaction of NO with peroxy radicals from VOC oxidation and O_3. NO_2 concentrations peak shortly before glyoxal levels do, and then decrease due to dilution of both gases in a rising boundary layer and chemical loss (i.e., photolysis, and HNO_3 formation for NO_2). Persisting glyoxal concentrations of about 1 ppbv around solar noon (Figure 1) reflect a photochemical loss rate of CHOCHO/$\tau_{min} = 0.75$ ppbv/hr be compensated by a comparable glyoxal production rate. The ratio of glyoxal to NO_2 reflects this active VOC chemistry until in the early afternoon increasing wind speeds indicate the ventilation of the MCMA (Figure 2c). During days of intense photochemical activity several ppbv of glyoxal are produced in the morning atmosphere within a few hours. Prior attribution of elevated morning levels of glyoxal as due to "emissions to ambient air" [*Kielhorn et al.*, 2004] not adequately reflect the intense source from VOC photochemistry, which is the dominant glyoxal source in the MCMA.

[12] Finally, the DOAS measurement of glyoxal opens the possibility for the use of existing satellite technology to better identify photochemical hot spots in the Earth's atmosphere. The absorption of glyoxal in the favourable visible wavelength range in principle allows detection by passive DOAS applications utilizing solar stray light (either ground- or airplane-based multi-axes (MAX-) DOAS or space-borne instruments). Feasibility of such detection can be assessed relative to tropospheric NO_2 columns that are routinely measured from space [*Velders et al.*, 2001; *Beirle et al.*, 2004]. The daytime glyoxal to NO_2 ratio in the MCMA ranges between 4.5–14% (8.1% on average during the campaign, Figure 2c). Tropospheric NO_2 columns above the MCMA have been measured $\sim 1.6 \times 10^{16}$ molec/cm^2, and 30–40% higher numbers are expected from existing satellites that use better spatial resolution [*Beirle et al.*, 2004]. The apparent differential optical density of glyoxal as viewed from space can be as high as 1.7×10^{-3} near 455 nm. This is above typical satellite sensor noise levels in this wavelength range and a detection of glyoxal from space seems feasible.

4. Conclusions

[13] Measurements of glyoxal (CHOCHO) by Differential Optical Absorption Spectroscopy (DOAS) are feasible on a routine basis in the Mexico City Metropolitan Area (MCMA) and other urban environments. The atmospheric residence time of glyoxal is considerably shorter than previously believed. For 'cloudless' days, glyoxal photolysis accounts for about two thirds of gas-phase glyoxal loss; OH-radical reactions are relatively more important in the presence of clouds, at elevated solar zenith angles (SZA > 80°), and at night.

[14] Glyoxal measurements present a very useful indicator molecule for volatile organic compound (VOC) chemistry. Glyoxal production rates are comparable during morning hours and overhead sun conditions, pointing out the importance of morning VOC oxidation processes for later smog formation. Time resolved DOAS measurements of glyoxal place a lower limit on the rate of VOC oxidation, and provide novel means to test predictions of smog formation by photochemical models.

[15] The detection of glyoxal by passive DOAS applications utilizing solar stray light in multi-axes (MAX-) DOAS or space-borne DOAS instruments seems feasible, and will allow infer information on VOCs not directly observable by these techniques. The use of glyoxal as an indicator for VOC chemistry is not limited to urban environments since glyoxal is formed from a variety of VOCs emitted by both anthropogenic and biogenic sources.

References

Alicke, B., et al. (2003), OH formation by HONO photolysis during the BERLIOZ experiment, *J. Geophys. Res.*, *108*(D1), 8247, doi:10.1029/2001JD000579.

Atkinson, R. (2000), Atmospheric chemistry of VOCs and NOx, *Atmos. Environ.*, *34*, 2063–2101.

Beirle, S., U. Platt, M. Wenig, and T. Wagner (2004), Highly resolved global distribution of tropospheric NO_2 using GOME narrow swath mode data, *Atmos. Chem. Phys.*, *4*, 1913–1924.

Calvert, J. G., R. Atkinson, J. A. Kerr, S. Madronich, G. K. Moortgat, T. J. Wallington, and G. Yarwood (Eds.) (2000), *The Mechanisms of Atmospheric Oxidation of the Alkenes*, Oxford Univ. Press, New York.

Calvert, J. G., R. Atkinson, K. H. Becker, R. H. Kamens, J. H. Seinfeld, T. J. Wallington, and G. Yarwood (Eds.) (2002), *The Mechanisms of Atmospheric Oxidation of Aromatic Hydrocarbons*, Oxford Univ. Press, New York.

Faloona, I. C., et al. (2004), A laser-induced fluorescence instrument for detecting tropospheric OH and HO_2: Characteristics and calibration, *J. Atmos. Chem.*, *47*, 139–167.

Fayt, C., and M. van Roozendael (2001), *WinDoas 2. 1–Software User Manual*, Belg. Inst. voor Ruimte Aëron.-Inst. d'Aéron. Spatiale Belg., Brussels.

Finlayson-Pitts, B., , and J. N. Pitts (Eds.) (2000), *Chemistry of the Upper and Lower Atmosphere*, Elsevier, New York.

Gregg, J. W., C. G. Jones, and T. E. Dawson (2003), Urbanization effects on tree growth in the vicinity of New York City, *Nature*, *424*, 183–187.

Grosjean, D., E. Grosjean, and A. W. Gertler (2001), On-road emissions of carbonyls from light-duty and heavy-duty vehicles, *Environ. Sci. Technol.*, *35*, 45–53.

Jang, M. S., N. M. Czoschke, S. Lee, and R. M. Kamens (2002), Heterogeneous atmospheric aerosol production by acid-catalyzed particle-phase reactions, *Science*, *298*, 814–817.

Kalberer, M., et al. (2004), Identification of polymers as major components of atmospheric organic aerosols, *Science*, *303*, 1659–1662.

Kean, A. J., E. Grosjean, D. Grosjean, and R. A. Harley (2001), On-road measurement of carbonyls in California light-duty vehicle emissions, *Environ. Sci. Technol.*, *35*, 4198–4204.

Kielhorn, J., C. Pohlenz-Michel, S. Schmidt, and I. Mangelsdorf (2004), Glyoxal, *Concise Int. Chem. Assess. Doc. 57*, Int. Programme on Chem.-Safety, World Health Org., Geneva.

Kraus, A., F. Rohrer, and A. Hofzumahaus (2000), Intercomparison of NO_2 photolysis frequency measurements by actinic flux spectroradiometry and chemical actinometry during JCOM97, *Geophys. Res. Lett.*, *27*, 1115–1118.

Molina, M. J., and L. T. Molina (Eds.) (2002), *Air Quality in the Mexico Megacity: An Integrated Assessment*, Springer, New York.

Platt, U. (1994), Differential optical absorption spectroscopy, in *Monitoring by Spectroscopic Techniques*, edited by M. W. Sigrist, chap. 2, pp. 27–84, John Wiley, Hoboken, N. J.

Plum, C. N., E. Sanhueza, R. Atkinson, W. P. L. Carter, and J. N. Pitts (1983), OH radical rate constants and photolysis rates of alpha-dicarbonyls, *Environ. Sci. Technol.*, *17*, 479–484.

Ramanathan, V., P. J. Crutzen, J. T. Kiehl, and D. Rosenfeld (2001), Aerosols, climate, and the hydrological cycle, *Science*, *294*, 2119–2124.

Sander, S. P., et al. (2002), Chemical kinetics and photochemical data for use in stratospheric modeling, *JPL Publ. 02–25*, *Evaluation Number 14*, Jet Propul. Lab., Calif. Inst. of Technol., Pasadena, Calif. (Available at http://jpldataeval.jpl.nasa.gov/)

Velders, G. J. M., C. Granier, R. W. Portmann, K. Pfeilsticker, M. Wenig, T. Wagner, U. Platt, A. Richter, and J. P. Burrows (2001), Global tropospheric NO_2 columns distributions: Comparing three-dimensional model calculations with GOME measurements, *J. Geophys. Res.*, *106*, 12,643–12,660.

Volkamer, R., U. Platt, and K. Wirtz (2001), Primary and secondary glyoxal formation from aromatics: Experimental evidence for the bicycloalkyl-radical pathway from benzene, toluene, and p-xylene, *J. Phys. Chem. A*, *105*, 7865–7874.

Volkamer, R., P. Spietz, J. P. Burrows, and U. Platt (2005), High-resolution absorption cross-section of Glyoxal in the UV/vis and IR spectral ranges, *J. Photochem. Photobiol. A*, doi:10.1016/j.jphotochem.2004.11.011, in press.

———————————

W. H. Brune and T. Shirley, Department of Meteorology, Pennsylvania State University, University Park, PA 16802, USA.

L. T. Molina, M. J. Molina, and R. Volkamer, Department of Earth Atmospheric and Planetary Sciences, MIT, 77 Massachusetts Avenue, Cambridge, MA 02139, USA. (rainer@alum.mit.edu)